Design of electron wave filters in monolayer graphene with velocity modulations*

Sun Li-Feng(孙立风)[a], Dong Li-Min(董利民)[b], and Fang Chao(房 超)[a]†

[a] Institute of Nuclear and New Energy Technology, Tsinghua University, Beijing 100084, China
[b] Beijing Key Laboratory of Fine Ceramics, Institute of Nuclear and New Energy Technology, Tsinghua University, Beijing 100084, China

(Received 24 September 2012; revised manuscript received 30 November 2012)

We compare the transport properties of electrons in monolayer graphene by modulating the Fermi velocity inside the barrier. A critical transmission angle is found only when the Fermi velocity in the barriers is larger than the one outside the barriers. It is shown that the transmission exhibits periodicity with the incident angle below the critical transmission angle, and attenuates exponentially in the opposite situation. For both situations, peak splitting occurs in the transmission as the number of the velocity barriers increases, and the characteristics of the transmission suggest an interesting application of an excellent band-pass filter. The dependence of the conductance on the Fermi energy through an identical velocity-modulation structure differs wildly with different Fermi velocities of the barrier. The counterpart of the peak splitting is the sharp oscillations in the conductance profile. Furthermore, some oscillations for the multiple barriers are so sharp that the structure may be used as an excellent sensor.

Keywords: velocity modulation, periodicity, peak splitting, sharp oscillations

PACS: 72.80.Vp, 73.23.Ad, 73.40.Gk **DOI:** 10.1088/1674-1056/22/4/047203

1. Introduction

A great amount of interest has been generated in research on the physical properties of graphene[1,2] since it was realized by Novoselov *et al.*[3] One reason for the intensive attention is that the charge carriers of graphene are massless and behave like the relativistic particles, then the transport of electrons and holes in such a truly two-dimensional (2D) material is governed by a massless Dirac equation. This brings about a number of unique electronic and transport properties, such as the unconventional quantum Hall effect,[4–8] the strong electric effect,[9] the finite minimal conductivity,[4,10] the special Andreev reflection,[11,12] and so on. Another reason for the intensive attention is that nanostructures based on graphene may have significant potential applications in nanoelectronics.[13] For example, the feature that the conductance near the Dirac point is very sensitive to the charge carriers density can be used to detect the absorption/desorption of a single molecule on graphene,[14] or sense small changes in the electric field and then the ionizing radiation.[15]

As we all know, the charge carriers at low energies of graphene can be described by a two-dimensional massless Dirac fermion model with the effective speed of light $v_F \approx 10^6$ m/s, as called the Fermi velocity.[16] Recently, researchers have shown that the Fermi velocity of charge carriers can be modulated by an appropriate doping,[17] placing a ground metal plane close to the graphene,[18] or imprinting a lateral superlattice with hexagonal symmetry on a two-dimensional electron gas.[19] It attracts interests in the velocity-modulation structures of graphene, because the velocity-modulation control in two different regions of graphene can be regarded as a velocity barrier.[20]

There have been some works on the transport properties through the velocity-modulation structures of graphene. Concha[20] first studied the effect of a velocity barrier on the ballistic transport of the Dirac fermions, and found the transmission is highly anisotropic. Then Yuan[21] investigated the guides modes in a symmetric velocity barrier, and found the velocity-controlled guiding of electron in graphene is an analogy of optical waveguides. Considering the electronic properties of graphene with velocity and potential barriers, it is found that the conductance exhibits periodic oscillations for the strong-velocity modulations.[22] When focusing on the tunneling of the Dirac fermions through a velocity barrier modulated by the magnetic fields, there is strong wave filtering and resonant effect in the transmission.[23]

However, there is no general and systematic conclusion about the change of the electronic transport properties under different velocity-modulations and it is necessary for us to understand the essence of electronic transport properties under this modulation. It is well known that the transport of an electron through semiconductor supperlattice would exhibit different features from the one through a single-barrier junction. Analogically, there should be remarkable similari-

*Project supported by the National Natural Science Foundation of China (Grant No. 11104156), the Postdoctoral Science Foundation of China (CPSF) (Grant No. 2012M510405), the Independent Research and Development Fund of Tsinghua University (Grant No. 20121087948), and Beijing Key Laboratory of Fine Ceramics Opening Fund (Grant No. 2012200110).

†Corresponding author. E-mail: fangchao@mail.tsinghua.edu.cn

© 2013 Chinese Physical Society and IOP Publishing Ltd

ties and differences between the transport properties through the complex velocity-modulation structures and those through the simple velocity-modulation structures. Furthermore, in order to obtain convictive results, the transport properties of Dirac fermions through various velocity-modulation structures in two different cases (Case 1: the Fermi velocity in the barrier is larger than the one outside; Case 2: the Fermi velocity inside smaller than the one outside) are considered in this article. It is found that there is periodicity and peak splitting in the transmission profile and some oscillations with falling-edge slopes are close to infinity in the conductance profile as the velocity barriers increased, which are firstly obtained and analyzed specifically. With these results, the potential applications based on these structures are also suspected and discussed preliminarily.

2. Model and method

We consider a graphene sheet in which the electron velocity varies in space, that is $v = v(\boldsymbol{r})$. Then the relevant Dirac equation with a space-dependent velocity is

$$v(\boldsymbol{r})\boldsymbol{\sigma}\cdot\boldsymbol{p}\Psi = E\Psi, \tag{1}$$

where $\boldsymbol{\sigma} = (\sigma_x, \sigma_y)$ is the standard Pauli matrix notation, and $\boldsymbol{p}$ is the momentum operator. Let us focus on a velocity barrier with a width D, which changes only along x direction as follows:

$$v(x) = \begin{cases} v_{\mathrm{F}}^0, & x < 0, \\ v_{\mathrm{F}}, & 0 \le x \le D, \\ v_{\mathrm{F}}^0, & x > D. \end{cases} \tag{2}$$

For simplicity, we define $n = v_{\mathrm{F}}/v_{\mathrm{F}}^0$ to describe different regions. In this case, $[p_y, H] = 0$, then the spinor wave function can be written as $\Psi(x,y) = (\psi_{\mathrm{I}}(x), \psi_{\mathrm{II}}(x))^{\mathrm{T}}\,\mathrm{e}^{\mathrm{i}k_y y}$ (T denoting the transpose of the row vector), where k_y is the perpendicular wave vector and remains invariable. To simplify the notation, we express all the quantities in the dimensionless units: $x \to x/D_0$, $E \to E/E_0$, $E_0 = \hbar v_{\mathrm{F}}^0/D_0$, where D_0 is the length unit and $v_{\mathrm{F}}^0 \approx 10^6$ m/s. For $D_0 = 10$ nm, $E_0 \approx 56.6$ meV. In these units, equation (1) is written explicitly as

$$\begin{pmatrix} -E/n & -\mathrm{i}\partial_x - \mathrm{i}k_y \\ -\mathrm{i}\partial_x + \mathrm{i}k_y & -E/n \end{pmatrix} \begin{pmatrix} \psi_{\mathrm{I}} \\ \psi_{\mathrm{II}} \end{pmatrix} = 0. \tag{3}$$

Then the first-order equation for the spinor components can be combined into a second-order equation

$$\left[\mathrm{d}^2/\mathrm{d}x^2 - k_y^2 + (E/n)^2\right]\psi_{\mathrm{I(II)}} = 0. \tag{4}$$

The solution to Eq. (4) can be obtained by writing the general solution in each region of the factor n as a linear combination (with complex coefficients) of the two independent elementary solutions first, and then imposing the continuity of the wavefunction at the interfaces between different regions to determine the complex coefficients. This procedure is conveniently performed in the transfer matrix formalism.[24,25] The wavefunction of the Dirac electrons in three regions with the incident energy E and the incident angle φ is given by

$$\psi_{\mathrm{I}} = \begin{cases} \mathrm{e}^{\mathrm{i}k_x x} + r\mathrm{e}^{-\mathrm{i}k_x x}, & x < 0, \\ a\mathrm{e}^{\mathrm{i}q_x x} + b\mathrm{e}^{-\mathrm{i}q_x x}, & 0 \le x \le D, \\ t\mathrm{e}^{\mathrm{i}k_x x}, & x > D, \end{cases} \tag{5}$$

$$\psi_{\mathrm{II}} = \begin{cases} \mathrm{e}^{\mathrm{i}\varphi}\mathrm{e}^{\mathrm{i}k_x x} - r\mathrm{e}^{-\mathrm{i}\varphi}\mathrm{e}^{-\mathrm{i}k_x x}l, & x < 0l, \\ a\mathrm{e}^{\mathrm{i}\theta}\mathrm{e}^{\mathrm{i}q_x x} - b\mathrm{e}^{-\mathrm{i}\theta}\mathrm{e}^{-\mathrm{i}q_x x}l, & 0 \le x \le Dl, \\ t\mathrm{e}^{\mathrm{i}\varphi}\mathrm{e}^{\mathrm{i}k_x x}l, & x > Dl, \end{cases} \tag{6}$$

where $k_x = \sqrt{E^2 - k_y^2} = E\cos\varphi$ and $q_x = \sqrt{(E/n)^2 - k_y^2} = E\cos\theta/n$ are the parallel wave vector components outside and inside the barrier, respectively.

In terms of the conversation of the energy and the perpendiculars wave vector k_y, for the graphene, we can obtain

$$\sin\theta = n\sin\varphi, \tag{7}$$

which is called Snell's law[26] and has the same physical mechanism as the conventional materials (with parabolic energy spectrum). Equation (7) implies that the electrons can travel through the barrier only if $|n\sin\varphi| \le 1$. When $|n\sin\varphi| > 1$, θ and the wave vector q_x are then imaginary, and the evanescent propagation appears in the barrier. Then the transmission is generally weak if the decaying length of the evanescent states is shorter than the barrier width. It will occur when $n > 1$ and the incident angle $|\varphi|$ is larger than the critical transmission angle $|\varphi_{\mathrm{c}}|$, which is equal to $|\arcsin(1/n)|$, but never occur when $n < 1$.

The boundary matching conditions can be inferred from the continuity equation $\nabla \cdot J(\boldsymbol{r}) = 0$, in the present work it means the divergence of the local current $J(x) = ev(x)\psi^{+}(x)\sigma\psi(x)$ vanishes, which leads to the following matching formulas

$$\begin{aligned} \sqrt{v_{\mathrm{F}}^0}\psi_1(0^-) &= \sqrt{v_{\mathrm{F}}}\psi_2(0^+), \\ \sqrt{v_{\mathrm{F}}}\psi_2(D^-) &= \sqrt{v_{\mathrm{F}}^0}\psi_3(D^+). \end{aligned} \tag{8}$$

According to the boundary conditions, the transmission probability can be obtained using the transfer matrix method. After getting the transmission probability, one can obtain the expression of the conductance. The zero-temperature conductance can be derived by integrating $\mathscr{T}$ over one-half of the (Fermi) energy surface

$$G(E) = G_0 \int_{-\pi/2}^{\pi/2} \mathscr{T}(E, E\sin\varphi)\cos\varphi\,\mathrm{d}\varphi, \tag{9}$$

where $G_0 = 2\mathrm{e}^2 E L_y/\pi h$. Here L_y is the length of the graphene sample in the y direction and G_0 includes a factor 4 coming from the spin and valley degeneracies.

3. Numerical results and discussion

Figure 1 compares the dependence of the transmission through various velocity-modulation structures on the incident energy for $n<1$ (Fig. 1(a)) and $n>1$ (Fig. 1(b)), with the incident angle smaller than the critical transmission angle. In this case, $|n\sin\varphi|<1$, then the transmission probability through a velocity barrier can be expressed by

$$\mathscr{T}_1=\left[1+\left(\frac{C}{B}\sin\mu_{\rm D}\right)^2\right]^{-1}, \tag{10}$$

where $B=\cos\theta\cos\varphi$, $C=\sin\varphi-\sin\theta$, and $\mu_{\rm D}=q_xD=ED\cos\theta/n$ is the phase for the wave propagating through a velocity barrier. Notice that Eq. (10) gives $\mathscr{T}_1=1$ for $\varphi=0°$, that is $C/B=0$, regardless of the values of other parameters, which is a manifestation of the Klein paradox in tunneling through a velocity barrier. The transmission reaches unity also for $\mu_{\rm D}=q_xD=m\pi$, and reaches to the minimum for $\mu_{\rm D}=q_xD=(m\pm1/2)\pi$, which corresponds to the peaks and the valleys of the transmission profile, respectively. The black lines in Figs. 1(a) and 1(b) indicate the transmission through a velocity barrier with the incident angle $\varphi=30°$ for $n<1$ and $n>1$, respectively. It is found that the transmission oscillates periodically with the incident energy increasing, which originates form the section $\sin\mu_{\rm D}$ in Eq. (10), and the period increases as n increases.

When electrons transport through the symmetric double barriers, and are well sandwiched between them, the transmission probability can be expressed by

$$\mathscr{T}_2=\left\{1+\left[2\frac{C}{B}\sin\mu_{\rm D}\left(\frac{A}{B}\sin\mu_{\rm D}\sin\mu_{\rm W}+\cos\mu_{\rm D}\cos\mu_{\rm W}\right)\right]^2\right\}^{-1}, \tag{11}$$

where $A=-1+\sin\theta\sin\varphi$, and $\mu_{\rm W}=k_xL$ is the phase through the well with a width L. The transmission probability not only depends on the propagation mode in the barriers, but also the mode in the well due to the coupling between the adjacent regions. It approaches unity when $C/B=0$, $\sin\mu_{\rm D}=0$, or $h=A/B\sin\mu_{\rm D}\sin\mu_{\rm W}+\cos\mu_{\rm D}\cos\mu_{\rm W}=0$, and reaches the minimum when $\mathrm{d}h/\mathrm{d}E=0$, which corresponds to the peaks and the valleys in the transmission profile, respectively.

As the red lines in Fig. 1 show, the transmission through the symmetric double barriers shows periodicity like $\mathscr{T}_1$, which originates from the section of $\sin\mu_{\rm D}$ and $\sin\mu_{\rm W}$ in Eq. (11). Then the period of the transmission profiles increases as n or φ increases. The difference of the transmission between $\mathscr{T}_1$ and $\mathscr{T}_2$ is that more peaks appear in $\mathscr{T}_2$, or rather, within a period each peak in $\mathscr{T}_1$ splits into two peaks in $\mathscr{T}_2$, regardless of the values of n, φ or E. The existence of these peaks at specific energy is characteristic of the resonant behavior in the velocity modulation structures, which is owing to the coupling between the barriers and the adjacent well and satisfies $\tan\mu_{\rm D}\tan\mu_{\rm W}=-B/A$.

With the increase of the number of the barriers, the periodicity still occurs in the transmission profile, as shown in Fig. 1. Similar to $\mathscr{T}_2$, within a period each peak in $\mathscr{T}_1$ broadens and splits into N peaks in the transmission through N barriers, and each valley becomes narrower and deeper. For large N (e.g., $N=40$), it is found that the valley turns into a gap, where the electrons are reflected perfectly. This suggests an interesting application of the structure as a band-pass filter, where only quasiparticles with energies within a certain limit can transmit.

As the incident angle increases (still smaller than the critical transmission angle), the characteristics of the transmission profile, such as the periodicity and the peak splitting, still occur. Comparing Fig. 1(a) with Fig. 2(a), it is found that the differences are the increase of the period of the transmission profile and the broadening of the gap with the increase of the incident angle.

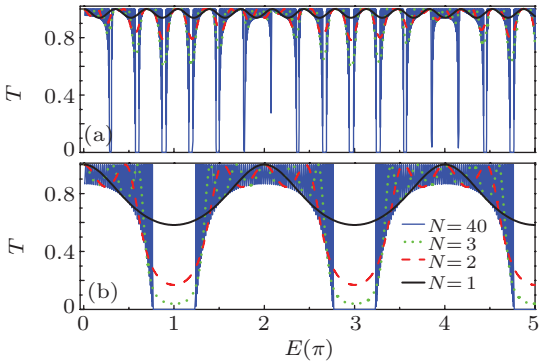


Fig. 1. (color online) Transmission through $N=1,2,3,40$ barriers as a function of the incident energy E, with (a) $n=1/\sqrt{3}$; (b) $n=\sqrt{3}$. $D=\sqrt{3}$, $L=1/\sqrt{3}$, and $\varphi=30°$. Note that the Fermi energy is labeled in π.

But when the incident angle exceeds the critical transmission angle, for example, $\varphi=36°>\varphi_{\rm c}=\arcsin(1/\sqrt{3})$, the angle θ and the wave vector q_x are imaginary, which indicates the evanescent propagation in the barriers. Moreover, the electrons will undergo lateral shifts along the interfaces of the barriers, as referred to Goos–Hänchen shift,[27,28] which depends on the deviation between the phase of the reflected (transmitted) wavefunction and the incident wavefunction. In the present work, we focus on the amplitude of the transmission coefficient and will not describe the effects related with the phase of the transmission coefficient in detail. We define $q_x=\mathrm{i}\kappa$, where $\kappa=\sqrt{(E/n)^2-k_y^2}$ is the decay constant. Then the transmission probability through a velocity barrier becomes

$$\mathscr{T}_1=\left[1-\left(\frac{C}{B}\sinh(\kappa D)\right)^2\right]^{-1}, \tag{12}$$

which attenuates exponentially as the function of the Fermi energy, as the black line shows in Fig. 2(b). And the transmission

through symmetric double barriers turns out to be

$$\mathscr{T}_2 = \left\{1 - \left[2\frac{C}{B}\sinh(\kappa D)\left(\frac{A}{B}\sinh(\kappa D)\sin\mu_W + \cosh(\kappa D)\cos\mu_W\right)\right]^2\right\}^{-1}, \quad (13)$$

which not only decays exponentially like $\mathscr{T}_1$, but also reaches unity when the Fermi energy satisfies $\tan(\kappa D)\tan\mu_W = -B/A$. Figure 2(b) shows the transmission through four velocity-modulation structures with the incident angle φ above the critical transmission angle φ_c. It is found that the transmission through multiple barriers is quite different from that through a velocity barrier, that is, the electrons with certain energy can transport perfectly through the former while decay to zero through the latter if the incident angle φ exceed the critical transmission angle φ_c. Furthermore, like in the case $\varphi < \varphi_c$, as the number of the velocity barriers increases, the peak splitting still exists and the positions of the gaps remain unchanged, but the differences in this case are that no periodicity exists and each peak in $\mathscr{T}_2$, rather than in $\mathscr{T}_1$, broadens and splits into $(N-1)$ peaks in the transmission through N barriers. This also possesses an application of an excellent band-pass filter based on the velocity-modulation structures.

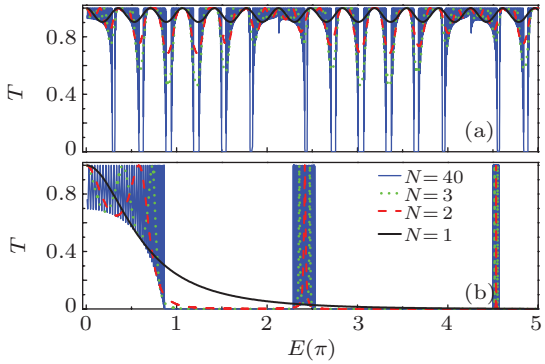


Fig. 2. (color online) Transmission through $N = 1,2,3,40$ barriers as a function of the incident energy E, with (a) $n = 1/\sqrt{3}$; (b) $n = \sqrt{3}$. $D = \sqrt{3}$, $L = 1/\sqrt{3}$, and $\varphi = 36°$. Note that the Fermi energy is labeled in π.

Figure 3(a) and 3(b) show the conductance through various velocity-modulation structures with $n < 1$ and $n > 1$, respectively. It is found that the conductance through the same velocity-modulation structure with different n is quite different as the Fermi energy increases. For the electrons transporting through a velocity barrier, the conductance oscillates periodically with the amplitudes decreasing when $n < 1$, but decays and approaches to a certain value when $n > 1$. In both $n < 1$ and $n > 1$ cases, as the number of the barriers increases, the trend of the conductance profile through multiple velocity barriers is the same as that through a velocity barrier, but some oscillations are found and the oscillations become sharper as the number of the velocity barriers increases, which agrees with the peak splitting in the transmission profile. More interestingly, when the number of the barriers are enough, for example, $N = 40$, the oscillations are so sharp that their falling-edge slopes approach infinity, which means the conductance here is very sensitive to the Fermi energy and the structure may be used to design an excellent switch.

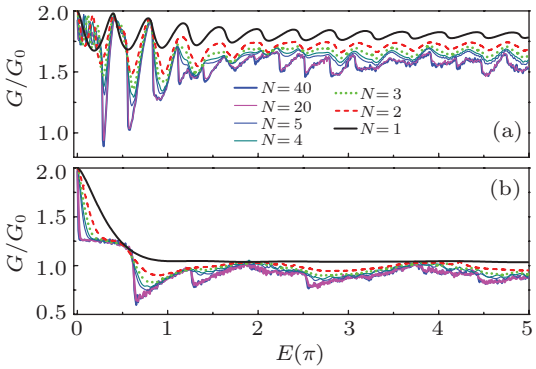


Fig. 3. (color online) The conductance in units of G_0 through $N = 1,2,3,4,5,20,40$ barriers as a function of the Fermi energy, with (a) $n = 1/\sqrt{3}$; (b) $n = \sqrt{3}$. $D = \sqrt{3}$, and $L = 1/\sqrt{3}$. Note that the Fermi energy is labeled in π.

4. Conclusion

In this paper, we compared the transport properties of electrons in the monolayer graphene by modulating the Fermi velocity of the barrier. It is found that there is a critical transmission angle only when the velocity in the barrier is larger than that outside the barrier ($n > 1$). When the incident angle is smaller than the critical transmission angle, the transmission through the velocity-modulation structures exhibits periodicity, and the period of the transmission profiles increases as the Fermi velocity of the barrier or the incident angle increases. However, when the incident angle exceeds the critical transmission angle, the transmission attenuates exponentially as a function of the incident energy, which only occurs when $n > 1$. In both cases, with the increase of the number of the velocity barriers, peak splitting occurs in the transmission and the characteristics of the transmission possess potential applications in resonant tunneling devices and energy filters. The dependence of the conductance through the velocity-modulation structure on the Fermi energy differs significantly with different n, that is, it oscillates periodically with the increase of the amplitudes when $n < 1$ but decays and approaches to a certain value when $n > 1$. The counterpart of the peak splitting in the transmission profile is the sharp oscillations in the conductance profile. Furthermore, some oscillations for the multiple barriers are so sharp that the structure may be used as an excellent sensor sensitive to the Fermi energy.

References

[1] Beenakker C W J 2008 *Rev. Mod. Phys.* **80** 1337

[2] Castro Neto A H, Guinea F, Novoselov K S and Geim A K 2009 *Rev. Mod. Phys.* **81** 109

[3] Novoselov K S, Geim A K, Morozov S V, Jiang D, Zhang Y, Dubonos S V, Grigorieva I V and Firsov A A 2004 *Science* **306** 666

[4] Novoselov K S, Geim A K, Morozov S V, Jiang D, Katsnelson M I, Grigorieva I V, Dubonos S V and Firsov A A 2005 *Nature* **438** 197

[5] Zhang Y B, Tan Y W, Stormer H L and Kim P 2005 *Nature* **438** 201

[6] Gusynin V P and Sharapov S G 2005 *Phys. Rev. Lett.* **95** 146801

[7] McCann E and Falko V I 2006 *Phys. Rev. Lett.* **96** 086805

[8] Zheng Y and Ando T 2002 *Phys. Rev. B* **65** 245420

[9] Zhang Y, Small J P, Amori M E S and Kim P 2005 *Phys. Rev. Lett.* **94** 176803

[10] Novoselov K S, McCann E, Morozov S V, Falko V I, Katsnelson M I, Zeitler U, Jiang D, Schedin F and Geim A K 2006 *Nat. Phys.* **2** 177

[11] Beenakker C W J 2006 *Phys. Rev. Lett.* **97** 067007

[12] Bhattacharjee S and Sengupta K 2006 *Phys. Rev. Lett.* **97** 217001

[13] Schwierz F 2010 *Nat. Nanotechnol.* **5** 487

[14] Schedin F, Geim A K, Morozov S V, Hill E W, Blake P, Katsnelson M I and Novoselov K S 2007 *Nat. Mater.* **6** 652

[15] Patil A *et al.* 2010 *IEEE Nuclear Science Symposium and Medical Imaging Conference*, October 30–November 6, 2010, Knoxville, TN, USA

[16] Katsnelson M I, Novoselov K S and Geim A K 2006 *Nat. Phys.* **2** 620

[17] Tapasztó L, Dobrik G, Nemes-Incze P, Vertesy G, Lambin Ph and Biró L P 2008 *Phys. Rev. B* **78** 233407

[18] Raoux A, Polini M, Asgari R, Hamilton A R, Fazio R and MacDonald A H 2010 *Phys. Rev. B* **81** 073407

[19] Gibertini M, Singha A, Pellegrini V, Polini M, Vignale G, Pinczuk A, Pfeiffer L N and West K W 2009 *Phys. Rev. B* **79** 241406

[20] Concha A and Tešanović 2010 *Phys. Rev. B* **82** 033413

[21] Yuan J H, Cheng Z, Zeng Q J, Zhang J P and Zhang J J 2011 *J. Appl. Phys.* **110** 103706

[22] Krstajić P M and Vasilopoulos P 2011 *J. Phys.: Condens. Matter* **23** 135302

[23] Yuan J H, Zhang J J, Zeng Q J, Zhang J P and Cheng Z 2011 *Physica B: Condens. Matter* **406** 4214

[24] McKellar B H J and Stephenson G J Jr 1987 *Phys. Rev. C* **35** 2262

[25] Barbier M, Peeters F M, Vasilopoulos P and Pereira J M 2008 *Phys. Rev. B* **77** 115446

[26] Zhang L B, Chang K, Xie X C, Buhmann H and Molenkamp L W 2010 *New J. Phys.* **12** 083058

[27] Wu Z H, Zhai F, Peeters F M, Xu H Q and Chang K 2011 *Phys. Rev. Lett.* **106** 176802

[28] Song Y, Wu H C and Guo Y 2012 *Appl. Phys. Lett.* **100** 253116